ELSEVIER

Journal of Nuclear Materials 257 (1998) 15–20

journal of nuclear materials

Thermotransport of hydrogen in Zircaloy-4 and modified Zircaloy-4

Hyun Seon Hong *, Seon Jin Kim, Kyung Sub Lee

School of Materials and Metallurgical Engineering, Hanyang University, 17 Haengdang-dong, Seoul 133-791, South Korea

Received 8 January 1998; accepted 8 May 1998

Abstract

Thermotransport of hydrogen, the flux of hydrogen due to an applied temperature gradient, was investigated in Zircaloy-4 and modified Zircaloy-4 alloys. The modified Zircaloy-4 was prepared by changing the chemical compositions of Zircaloy-4. The heat of transport (Q^*) for hydrogen was determined to evaluate the magnitude and direction of thermotransport in the alloys, and the hydrogen distribution induced by thermotransport was investigated. During the thermotransport hydrogen existed in two different regions, the single-phase region and the two-phase region. At the interface between the two different regions, the hydrogen concentration distribution did not show a sharp discontinuity but a relatively smooth curve. The values for Q^* in Zircaloy-4 and modified Zircaloy-4 alloys were considered to be about 30 kJ/mol.

1. Introduction

Recently a modified Zircaloy-4 alloy was developed by changing the chemical composition of Zircaloy-4. The tin contents decreased from 1.0 to 0.5 wt% and zero while oxygen increased from 0.1 to 0.8 wt%. 0.1 wt% Nb was added and the amounts of Fe and Cr were kept 0.1 and 0.2 wt% respectively. The oxygen addition caused a marked improvement in the mechanical strength, and the modified Zircaloy-4 containing 0.2 wt% oxygen showed a better oxidation resistance than that of Zircaloy-4 [1]. The recent trends toward extended burn-up and high pH operation result in hydrogen redistribution during operation which is one of the problems associated with the use of Zircaloy-4 in pressurized water reactors (PWRs). Thus, it is necessary to investigate the characteristics of hydrogen redistribution in the modified Zircaloy-4 in addition to tensile and oxidation properties.

Hydrogen, resulted mainly from the oxidation reaction of Zircaloy-4, is absorbed by the claddings during operation of PWRs [2,3]. Under the influence of a temperature gradient, hydrogen in Zircaloy-4 move towards the colder regions until the steady state condition is established [4,5]. Hydrogen precipitates as zirconium hydrides at the cold end due to the low solubility of hydrogen in Zircaloy-4. Because precipitates of zirconium hydride in Zircaloy-4 can have pronounced effects on the mechanical properties, it is important to know the hydrogen redistribution, i.e., thermotransport of hydrogen under a temperature gradient. Sawatzky [6] studied this phenomenon extensively in out-pile tests and developed models to describe it. However Sawatzky's model is not suited to describe the thermotransport likely to be encountered in reactors where the shallow temperature difference (300–340°C) is applied to the claddings.

In the present study, the thermotransport of hydrogen in Zircaloy-4 and in modified Zircaloy-4 for the temperatures likely to be encountered in reactors was investigated. The heat of transport (Q^*) for hydrogen was determined. The magnitude of the thermotransport and the effect of oxygen on the value of Q^* were investigated. The hydrogen concentration distribution induced by the thermotransport was also examined. With these experimental data the kinetics for the thermotransport in Zircaloy-4 and the modified Zircaloy-4 were discussed.

* Corresponding author.

0022-3115/98/$ – see front matter
PII: S0022-3115(98)00430-9

2. Equations

2.1. Hydrogen distribution at steady state

The theoretical basis of the thermotransport has been discussed in a number of literature [7–11]. The basic idea of the theory is that in the presence of a temperature gradient an atomic flux can occur. The atomic flux is given by Denbigh [12] as

$$J = \frac{-DC}{RT}\left\{RT\frac{\mathrm{d}\ \ln\ \mathrm{C}}{\mathrm{d}x} + \frac{Q^*}{T}\frac{\mathrm{d}T}{\mathrm{d}x}\right\}, \tag{1}$$

where D is the diffusion coefficient, C the hydrogen concentration, T the temperature, R the gas constant, Q^* the heat of transport and x the coordinate through the diffusion region.

A steady state is reached when the flux caused by the concentration gradient equals that caused by the temperature gradient. Under this condition the net flow vanishes ($J=0$) and Eq. (1) can be written

$$\frac{\mathrm{d}\ \ln\ C}{\mathrm{d}(1/T)} = \frac{Q^*}{R}. \tag{2}$$

It is seen that the value of the heat of transport (Q^*) is obtained from Eq. (2).

The hydrogen distribution at the steady state can be obtained by integrating Eq. (2). This leads to

$$C = A\ \exp(Q^*/RT), \tag{3}$$

where A is a constant. The value of constant A is determined by the boundary condition where the hydrogen is conserved, i.e.,

$$\frac{1}{a}\int_0^a C\,\mathrm{d}x = C_0, \tag{4}$$

where C_0 is the original concentration of hydrogen and a is the length of the specimen. On introducing Eq. (3), Eq. (4) becomes

$$A = \frac{aC_0}{\int_0^a \mathrm{e}^{Q^*/RT}\mathrm{d}x}. \tag{5}$$

Consequently, the hydrogen distribution at the steady state, induced by the thermotransport, can be determined from Eq. (3) with the value of A calculated in Eq. (5).

2.2. Time to steady state

The time required to attain the steady state hydrogen distribution can be given approximately as the time required for all the hydrogen to be precipitated out as hydride at the cold surface according to Sawatzky's model [6]:

$$t_\mathrm{s} = C_0\frac{a}{J(T_\mathrm{C})}. \tag{6}$$

In Eq. (6), C_0 is the initial hydrogen concentration and a is the length of the specimen. $J(T_\mathrm{C})$ is the flux of hydrogen at the cold surface which may be calculated from Eq. (1) as follows.

If the solid solution at every point in a temperature gradient is assumed to be in equilibrium with hydride, the hydrogen concentration in the solid solution is equal to the terminal solid solubility at the corresponding temperature [13],

$$C = C_\mathrm{s} = C_0\ \exp(-\Delta H/RT), \tag{7}$$

where C_s is the terminal solid solubility, C_0 the constant and ΔH the heat of mixing of hydrogen in alpha zirconium.

On differentiating with x, a coordinate, Eq. (7) may be given as

$$RT\frac{\mathrm{d}\ \ln\ C}{\mathrm{d}x} = \frac{\Delta H}{T}\frac{\mathrm{d}T}{\mathrm{d}x}. \tag{8}$$

Upon substitution of Eq. (8) into the first term in the brackets of Eq. (1),

$$J(T_\mathrm{C}) = \frac{DC}{RT_\mathrm{C}^2}\{\Delta H + Q^*\}\frac{\mathrm{d}T}{\mathrm{d}x}. \tag{9}$$

The value of ΔH has been determined to be 36.1 kJ/mol by Gulbransen [14]. Mallett [15] gives D as a function of temperature. Thus, the time to steady state is obtained from Eq. (6), using the calculated value of $J(T_\mathrm{C})$ and the experimental constants a and C_0.

3. Experimental procedure

The sheet type specimens for the thermotransport test with dimensions of 30 mm (L) × 8 mm (W) × 0.6 mm (t) were prepared by the procedures described in the previous study [1]. The chemical compositions of the specimens for the thermotransport test are presented in Table 1.

The sheet specimens were mechanically polished and then electropolished in a solution of 15 vol.% $HClO_4$ + 85 vol.% acetic acid. Hydrogen was introduced into the electropolished specimens by means of electrolytic cathodic charging. A platinum anode and an electrolyte of 10 vol.% H_2SO_4 + 90 vol.% H_2O were used for the cathodic charging. Hydrogen was charged for 60 s at 80°C with a current density of 4 A/m^2. The initial hydrogen contents by the cathodic charging were 57.4 and 59.4 ppm by weight in the 0.5Sn–0.1O–Zr and 0.5Sn–0.2O–Zr specimens, respectively. These specimens were used for the thermotransport test for 100 days. The initial hydrogen contents were 88.3 and 85.0 ppm in the Zircaloy-4 and 0.5Sn–0.1O–Zr specimens, respectively, used for the 50 days test. After charging, the specimens were homogenized at 340°C for 20 days in order to ensure that the hydrogen concentration was uniform in the specimens.

Table 1
Chemical compositions of Zircaloy-4 and the modified Zircaloy-4 alloys for the thermotransport tests (wt%)

Specimens	Alloying elements					
	Sn	Nb	Cr	Fe	O	Zr
#1	0.5	0.1	0.2	0.1	0.1	Bal.
#2	0.5	0.1	0.2	0.1	0.2	Bal.
#3 (Zry-4)	1.2–1.7	0.01	0.07–0.13	0.18–0.24	0.09–0.16	Bal.

The hydrogen-charged specimen was placed in tube furnaces with one end of the specimen at 340°C and the other at 300°C. A preliminary run with three chromel–alumel thermocouples equally spaced along the specimen indicated a constant temperature gradient.

After sufficient time (100 days) to reach a steady state condition of the hydrogen distribution, the specimen was removed and cut into slices of equal size. These slices were analyzed for hydrogen by the hot vacuum extraction method, and the hydrogen distribution along the specimen was determined.

The time to steady state (t_s) was calculated to be 90 days from Eq. (6), using $C_0 = 57.4$ ppm by weight, $a = 2.4$ cm, $\Delta H = 36.1$ kJ/mol [14], $D_H = 8.3 \times 10^{-11}$ m^2/s [15], and $Q^* = 30$ kJ/mol as obtained in the present study.

4. Results and discussion

The hydrogen distribution in the 0.5Sn–0.1O–Zr and 0.5Sn–0.2O–Zr specimens after the thermotransport test for 100 days is shown in Fig. 1. In the 0.5Sn–0.1O–Zr specimen, the hydrogen concentration at the hot end of the specimen decreased from 57.4 to 36.9 ppm. At the cold end, the concentration increased from 57.4 up to 115.5 ppm, and the concentration was higher than the terminal solubility limit for the temperature of the cold end. The terminal solubility line was drawn from data by Kearns [16]. Thus, it was considered that hydrogen was transported from the hot end to the cold end, and the hydride precipitation occurred at the cold end as a result of thermotransport. The 0.5Sn–0.2O–Zr specimen showed the similar result to the 0.5Sn–0.1O–Zr specimen as shown in Fig. 1.

In Fig. 1, the experimental hydrogen distributions are compared to the theoretical ones. The agreement between experiment and theory is seen to be good in the single-phase region as shown in Fig. 1. The theoretical hydrogen distribution was determined from Eq. (3) with the calculated value of A in Eq. (5). The integration required in Eq. (5) was performed numerically using the values $Q^* = 30$ kJ/mol as measured in this study and $dT/dx = 16$ K/cm, and the value of A was calculated by using $a = 2.4$ cm and $C_0 = 57.4$ ppm by weight. The experimental hydrogen concentration near the cold end side is much higher than the theoretical one because the experimental hydrogen is a sum of the amount of hydrogen in solid solution and in the form of hydride, while the theoretical hydrogen concentration is the amount of hydrogen only in solid solution.

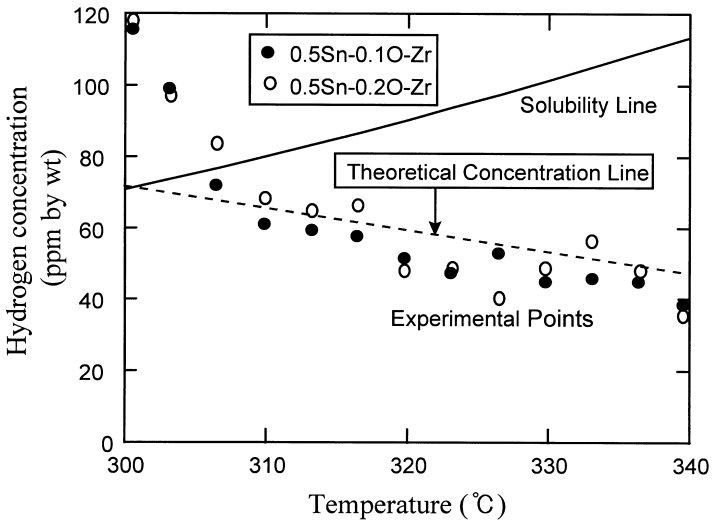

Fig. 1. Hydrogen distribution in 0.5Sn–0.1O–Zr and 0.5Sn–0.2O–Zr specimens after 100 days.

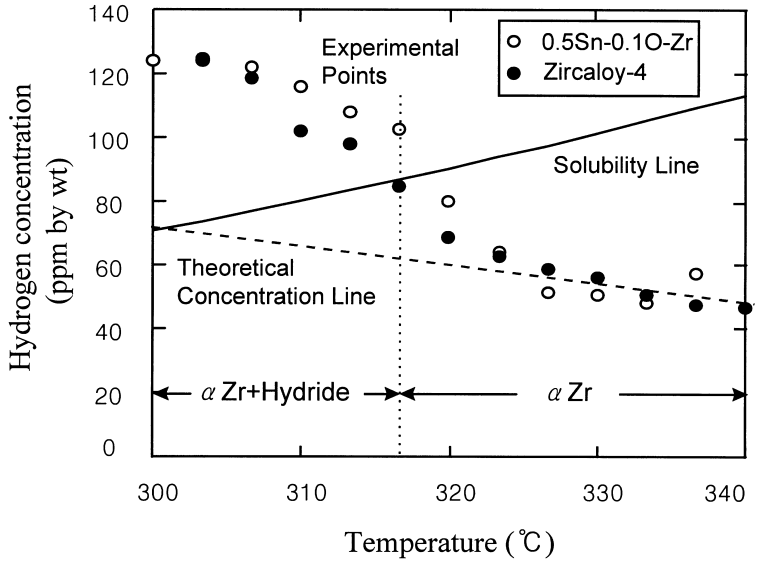

Fig. 2. Hydrogen distribution in Zircaloy-4 and 0.5Sn–0.1O–Zr specimens after 50 days.

Fig. 2 is the hydrogen distribution in Zircaloy-4 and 0.5Sn–0.1O–Zr specimens for 50 days, which is not sufficiently long enough to allow the hydrogen to reach a steady state distribution. The theoretical hydrogen distribution is also given. The experimental points of hydrogen concentration in the single-phase region show good agreement with the theoretical hydrogen concentration distribution.

Fig. 2 shows the single-phase region in which hydrogen exists in alpha zirconium as a solid solution, and the two-phase region in which alpha solid solution and zirconium hydride coexist. The hydrogen distribution showed a relatively smooth curve at the interface between the single-phase region and the two-phase region, that is, a relatively small increase in concentration at the interface. However, Sawatzky [6] reported an abrupt increase in concentration at the interface before steady state was reached. The increase in the hydrogen concentration was much higher than that in the present study. In Sawatzky's experiment, the temperature difference between the hot and cold ends of the specimen was larger than that of the present experiment. In a large temperature difference, a great amount of hydrogen accumulated as hydride at the interface so that an abrupt increase in concentration could result at the interface in Sawatzky's experiment.

In Fig. 2, the hydrogen concentration in the two-phase region increased with decreasing temperature. However, in contrast to the results presented in Fig. 2, the hydrogen concentration decreased with decreasing temperature, showing a maximum hydrogen concentration at the interface, in Sawatzky's experiment. The diffusivity of hydrogen at the temperature of the hot end side is about 3 orders larger than at the temperature of the cold end side in Sawatzky's experiment, while two times larger in the present study. The diffusivity difference in Sawatzky's is much higher than in the present study. Sawatzky's hydrogen concentration profile in the two-phase region could result from the large diffusivity difference. In a large diffusivity difference, the colder region in the two-phase region gains hydrogen at a slower rate than hydrogen moves away from the interface and so the hydrogen concentration in the two-phase region will decrease with decreasing temperature. However, if each point in the two-phase region gains hydrogen at an almost same rate in a shallow temperature difference as in the present study, the hydrogen concentration in the two-phase region will increase with decreasing temperature due to an almost constant hydrogen gaining rate at every point in the two-phase region.

Consequently, it is considered that temperature difference between the hot and cold ends of the specimen determines the shape of the hydrogen distribution. A larger temperature difference causes a sharp discontinuity in the concentration (an abrupt increase in the concentration at the interface and a decrease in the concentration with decreasing temperature at the two-phase region), while a relatively smooth hydrogen concentration curve is obtained in which a small temperature difference is applied.

Fig. 3 represents the logarithmic plot of hydrogen concentration as a function of temperature, drawn to determine the value of Q^* for the 100 days test. The value for Q^* of 29 kJ/mol was obtained for the 0.5Sn–0.1O–Zr specimen and 32.7 kJ/mol for the 0.5Sn–0.2O–Zr specimen. Values ranging from 27.6 to 29.8 kJ/mol [17] were reported in zirconium and 25.2 kJ/mol for

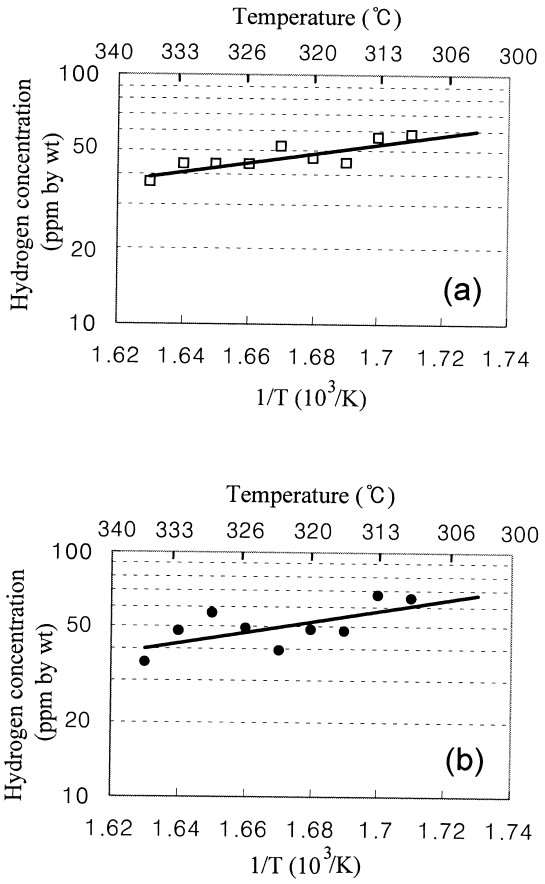

Fig. 3. Logarithmic plot of hydrogen concentration as a function of the inverse temprature for the 100 days test. (a) 0.5Sn-0.1O–Zr; (b) 0.5Sn–0.2O–Zr.

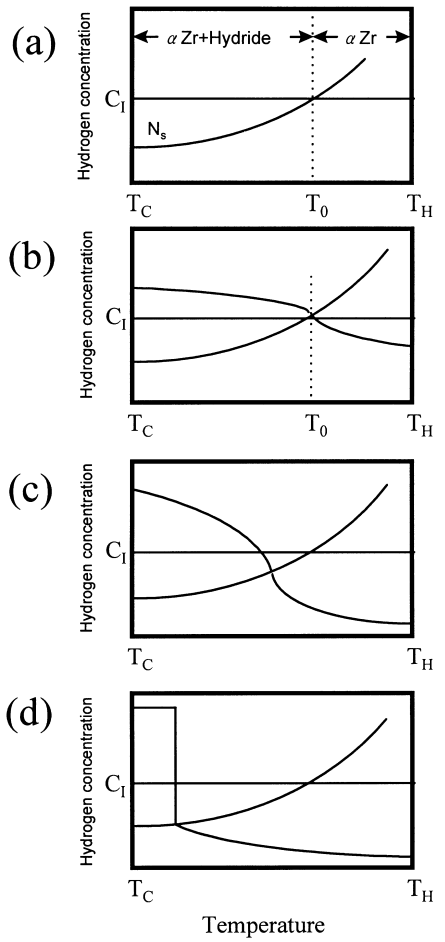

Fig. 4. Schematic diagram of hydrogen distribution. (a) Initial uniform hydrogen distribution; (b) Hydrogen distribution sometime before steady state has been achieved; (c) Hydrogen distribution at intermediate stage; (d) Final hydrogen distribution at steady state.

Zircaloy-2 by Sawatzky [6]. In the present study, the value of Q^* was obtained by the least-squares regression method (using a statistical program of S-PLUS 4 version) and 'multiple R-squared' was calculated to be about 0.72. This means that the experimental data points in Fig. 3 deviate from the line obtained by the least-squares regression by 28%. In the present 100 days test, the value of Q^* for the 0.5Sn–0.2O–Zr specimen (32.7 kJ/mol) was higher than that of the 0.5Sn–0.1O–Zr specimen (29 kJ/mol). However, it is statistically meaningless to compare the values of Q^* because the difference in the values fell within the statistical error range.

In Fig. 2, the experimental points of hydrogen concentration in the single-phase region show good agreement with the theoretical ones. The heats of transport of 28.1 and 29.8 kJ/mol for the Zircaloy-4 and 0.5Sn–0.1O–Zr specimens, respectively, were estimated from the single-phase regions for the 50 days test. Values for Q^*, as obtained in the present investigation, were 28.1 and 29.8 kJ/mol for the 50 days test, and were 29 and 32.7 kJ/mol for the 100 days test. Thus, the heat of transport for hydrogen in Zircaloy-4 and the modified Zircaloy-4 specimens is considered to be about 30 kJ/mol.

The schematic diagrams of the process of thermotransport in the present specimens are shown in Fig. 4. Fig. 4(a) illustrates that the initial hydrogen concentration is uniform and the concentration is higher than the terminal solubility in the colder region. N_s represents the terminal solubility line and C_I the initial uniform hydrogen concentration. T_C and T_H are the temperatures at the cold and hot ends of the specimens. T_0 is the temperature at the initial position of the interface between the single-phase region and the two-phase region. When thermotransport of hydrogen begins in the solid solution, the gradient of concentration is established as shown in Fig. 4(b). The hydrogen moving away from the hot end region would tend to accumulate as hydride at

the interface between the single-phase and the two-phase region. As the thermotransport proceeds to a stage beyond a stage of Fig. 4(b), the hydride initially present at T_0 in Fig. 4(b) begins to dissociate and go into solid solution; as hydrogen in solid solution moves from the interface at T_0 to the colder region by the thermotransport, the hydrogen concentration in the solid solution at T_0 becomes lower than the solubility limit for the temperature of T_0. The solid solution is assumed to be in equilibrium with the hydride at T_0. Thus, the hydride would dissociate and go into solid solution to maintain an equilibrium at T_0.

The diffusion rate in the single-phase region is higher than in the two-phase region, so that a steady state hydrogen distribution will first be achieved in the single-phase region. As the thermotransport proceeds, the interface between the single-phase and the two-phase region moves toward the colder surface. Hydride precipitation and dissolution at the moving interface are repeated until the steady state is reached. Ultimately the hydride must precipitate at the cold end of the specimen through an intermediate stage of Fig. 4(c) as shown in Fig. 4(d). The schematic concentration profile in Fig. 4(c) is drawn from the result of the thermotransport test for 50 days shown in Fig. 2 and that in Fig. 4(d) for the 100 days test shown in Fig. 1.

5. Conclusions

1. Hydrogen moved away from the hot end region of the specimen and accumulated as hydride at the cold end of the specimen as a result of thermotransport. During thermotransport hydrogen existed in two different regions, the single-phase region and the two-phase region.

2. The hydrogen distribution showed a relatively smooth curve at the interface between the two different regions, instead of showing a sharp discontinuity. It was thought that the temperature difference between the hot and cold ends of the specimen determined the shape of the hydrogen distribution during thermotransport.

3. In the steady state, the heats of transport (Q^*) in Zr–0.5Sn0–0.1O and Zr–0.5Sn–0.2O were 29 and 32.7 kJ/mol, respectively. The Q^* values of 28.1 and 29.8 kJ/mol for Zircaloy-4 and 0.5Sn–0.1O–Zr respectively, were estimated from the single-phase regions in the 50 days test. Thus, the heat of transport for hydrogen in the present study is considered to be about 30 kJ/mol.

References

[1] Hyun Seon Hong, Seon Jin Kim and Kyung Sub Lee, J. Nucl. Mater. 238 (1996) 211.
[2] M.G. Fontana, Advances in Corrosion Science and Technology, Plenum, New York, USA, 1976.
[3] A. Sawatzky and M. Duclos, Trans. Metall. Soc. AIME 245 (1969) 831.
[4] B.J.S. Wilkins and A. Wasylyshyn, J. Nucl. Mater. 29 (1969) 235.
[5] K. Forsberg and A.R. Massih, J. Nucl. Mater. 172 (1990) 30.
[6] A. Sawatzky, J. Nucl. Mater. 2 (1960) 321.
[7] S.R. DeGroot, Thermodynamics of Irreversible Processes, North-Holland, Amsterdam, 1951.
[8] G. Alefeld and J. Völkl, Hydrogen in Metals, Springer, Berlin, 1978.
[9] P. Shewmon, Diffusion in Solids, The Minerals, Metals and Materials Society, Pennsylvania, 1989.
[10] H. Wipf and F. Alefeld, Phys. Stat. Sol. 23 (1974) 175.
[11] R.A. Oriani, J. Phys. Chem. Solids. 30 (1969) 339.
[12] K.G. Denbigh, The Thermodynamics of the Steady State, Methuen Monograph, London, 1951.
[13] P.G. Shewmon, Trans. Met. Soc. AIME 212 (1958) 642.
[14] E.A. Gulbransen and K.F. Andre, Trans. Am. Inst. Mining Met. Eng. 203 (1955) 136.
[15] M. Mallett and W. Albricht, J. Electrochem. Soc. 104 (1957) 142.
[16] J.J. Kearns, J. Nucl. Mater. 22 (1967) 292.
[17] J.M. Markowitz, Westinghouse Atomic Power Division (USA) Report, WAPD-TM-104 (1958).